Article

Following Molecular Mobility during Chemical Reactions: No Evidence for Active Propulsion

Lucy L. Fillbrook, Jan-Philipp Günther, Günter Majer, Daniel J. O'Leary, William S. Price, Hal Van Ryswyk, Peer Fischer,* and Jonathon E. Beves*

ACCESS | Metrics & More | Article Recommendations | Supporting Information

ABSTRACT: The reported changes in self-diffusion of small molecules during reactions have been attributed to "boosted mobility". We demonstrate the critical role of changing concentrations of paramagnetic ions on nuclear magnetic resonance (NMR) signal intensities, which led to erroneous measurements of diffusion coefficients. We present simple methods to overcome this problem. The use of shuffled gradient amplitudes allows accurate diffusion NMR measurements, even with time-dependent relaxation rates caused by changing concentrations of paramagnetic ions. The addition of a paramagnetic relaxation agent allows accurate determination of both diffusion coefficients and reaction kinetics during a single experiment. We analyze a copper-catalyzed azide−alkyne cycloaddition "click" reaction, for which boosted mobility has been claimed. With our methods, we accurately measure the diffusive behavior of the solvent, starting materials, and product and find no global increase in diffusion coefficients during the reaction. We overcome NMR signal overlap using an alternative reducing agent to improve the accuracy of the diffusion measurements. The alkyne reactant diffuses slower as the reaction proceeds due to binding to the copper catalyst during the catalytic cycle. The formation of this intermediate was confirmed by complementary NMR techniques and density functional theory calculations. Our work calls into question recent claims that molecules actively propel or swim during reactions and establishes that time-resolved diffusion NMR measurements can provide valuable insight into reaction mechanisms.
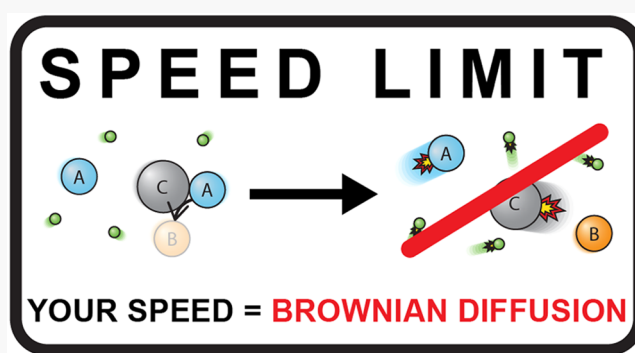
■ INTRODUCTION

Motion at the molecular level[1] is central for the development of molecular machines and devices.[2] Biology is rich in examples of active movement in molecular systems, which provide inspiration for synthetic chemical analogues.[1c,d,f] The diffusive motion of molecular species can be monitored by dynamic light scattering,[3] fluorescence correlation spectroscopy,[4] or nuclear magnetic resonance (NMR) spectroscopy.[5] Diffusion NMR provides information about molecular motion and can be used to determine the size and diffusive properties of molecules and enzymes[6] *in situ* and noninvasively.[7]

Diffusion NMR has been used to argue that molecular species involved in chemical reactions display mobility higher than passive Brownian motion.[8] The energy released during the reaction was claimed to directly propel the molecule (displayed schematically in Figure 1a).[8] Such a phenomenon would have tremendous implications for our fundamental understanding of chemical reactions. However, there is currently no theoretical explanation that supports these observations.[1f] The first example to claim enhanced diffusion of small molecules during a catalyzed reaction involved a Grubbs metathesis catalyst,[9] although this was later found to

be due to convection artifacts.[10] More recently, it has been claimed that an increase in molecular mobility during reactions is a general phenomenon, as purportedly the reactants and the solvent show enhanced diffusion in a number of chemical reactions.[8] In the most spectacular example,[8] a reactant in a copper-catalyzed azide−alkyne cycloaddition (CuAAC) "click" reaction (Figure 1b) showed an apparent 60% increase in its diffusion coefficient, while the diffusion coefficient of the residual solvent had an apparent 20% increase. We re-examined this experiment and concluded that there is no enhanced diffusion,[11] while the authors maintain their claims.[12]

Herein we outline factors that can affect diffusion NMR measurements of dynamic systems involving changing concentrations of paramagnetic species, which is the case for the CuAAC reaction. We show that the addition of an inert
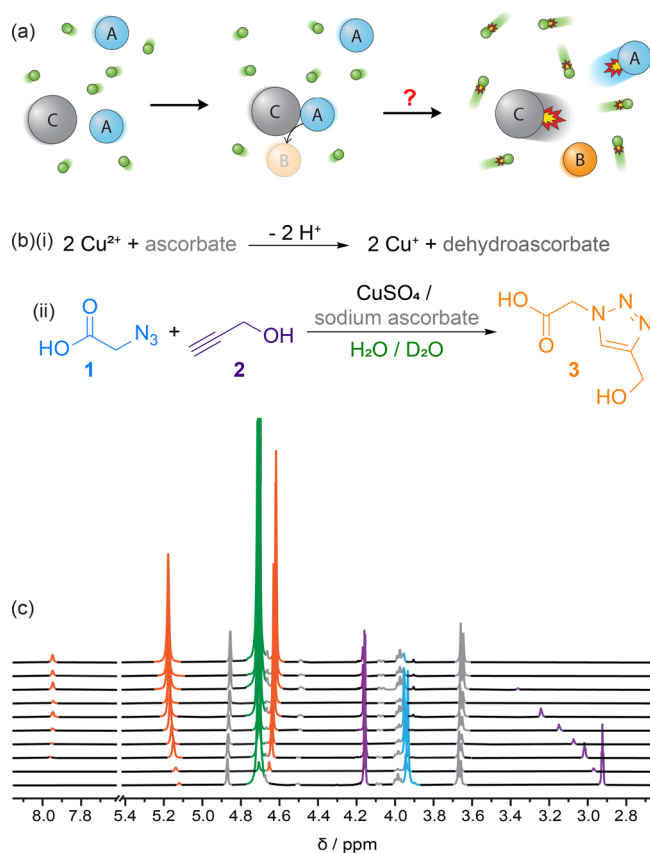
Figure 1. Enhanced diffusion during the CuAAC reaction? (a) Proposed "boosted mobility": catalyst C converts species A to B while surrounded by solvent (green). The energy released during the reaction has been claimed to lead to increased (active) diffusion of all species, including solvent and reactant.[8,13] (b) Reaction scheme for (i) the redox reaction between copper(II) and ascorbate[14] and (ii) the CuAAC reaction studied. (c) Representative spectra from a diffusion ^{1}H NMR experiment during the reaction.

paramagnetic relaxation agent, in modest concentrations, can allow simultaneous measurement of accurate diffusion coefficients and kinetics, which is otherwise not possible. The results have been verified independently by three laboratories using different types of NMR probes, acquisition methods, and reagent sources (SI-8.4).

■ RESULTS AND DISCUSSION

Pulsed gradient spin-echo (PGSE) or stimulated-echo (PGSTE) NMR[5] can simultaneously measure the self-diffusion coefficient, D, and concentration of different molecular species. The measured NMR signal intensity, I, for the PGSE sequence is given by the Stejskal−Tanner equation:[15]

$$I = I_0 \exp\left[-D\gamma^2 g^2 \delta^2\left(\Delta - \frac{1}{3}\delta\right)\right] = I_0 \exp[-Db] \tag{1}$$

where I_0 is the NMR signal intensity in the absence of the applied gradient (ideally proportional to concentration), γ is the gyromagnetic ratio of the nucleus, g and δ describe the amplitude and duration of the magnetic field gradient pulse, respectively, and the delay Δ defines the timescale over which diffusion is measured. Estimates of D and I_0 are determined by nonlinear regression of eq 1 onto the data. In dynamic systems,

factors other than g that influence the signal intensity during the measurement lead to processing and analysis problems.[16]

During chemical reactions, concentration changes lead to time-dependent I_0 values. If the changes in concentration are correlated to the order of the gradient pulse amplitudes applied in a diffusion NMR experiment, the diffusion coefficient will be miscalculated (SI-8.3, SI-13).[17] A less obvious factor that influences I_0 is the relaxation rate,[18] i.e., changes in the longitudinal relaxation time constant (T_1) or transverse relaxation time constat (T_2). Both T_1 and T_2 are influenced by the local environment and dynamics of the nucleus being observed and thus depend on factors like viscosity and the presence of paramagnetic species.[18]

The T_1 of HDO in D$_2$O is well-known to depend on the concentration of paramagnetic ions such as copper(II)[18] or gadolinium(III).[19] Typical data shown in Figure 2 demonstrate
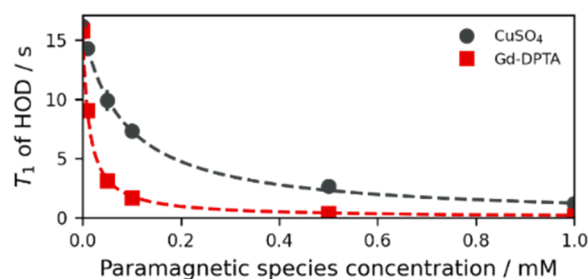

Figure 2. Dependence of longitudinal relaxation constant, T_1, on the concentration of paramagnetic ions. T_1 of the residual HDO peak with varying CuSO$_4$ or gadolinium−diethylenetriaminepentaacetic acid (Gd-DTPA) concentration, obtained by inversion recovery experiments (^{1}H NMR 500 MHz, 298 K, 12 relaxation delays ranging from 0.1 ms to 120 s, depending on the expected T_1). Dashed lines: $T_1 = 1/(a + b[M])$, where $[M]$ is the concentration of the paramagnetic species.[18,20] Data are in agreement with first reports.[18,19]

that changes in very low concentrations of copper(II) ions result in significant changes in T_1 relaxation. We find the T_1 for HDO changes from 15 ± 1 s in D$_2$O (SI-5.1) to 1.2 ± 0.1 s at just 1 mM copper(II) sulfate (SI-5.3), consistent with earlier reports.[18] This is important as very small (i.e., catalytic) concentrations of copper(II) ions will result in substantial changes in the relaxation rates of HDO and all species in solution.

We now consider the T_1 of HDO during the CuAAC reaction (Figure 1b). In the initial stages of the reaction, paramagnetic copper(II) is reduced to the catalytically active copper(I), dramatically changing the T_1 of HDO.[21] We find that in a D$_2$O solution of 250 mM azide **1** and 250 mM alkyne **2** the T_1 of HDO is 12 ± 2 s, as measured by inversion recovery experiments (SI-5.5).[22] The addition of 20 mM copper(II) sulfate shortened the T_1 to just 69 ± 4 ms[23]—a ~190-fold change (SI-5.6).[24] These results indicate that the T_1 of HDO can change by two orders of magnitude as paramagnetic copper(II) is reduced to copper(I). We verified these changes by measuring the time-resolved T_1 during the CuAAC reaction using saturation recovery NMR experiments (Figure 3a and SI-6). If the changing T_1 is correlated to a monotonic order of gradient amplitudes used in the diffusion experiment,[8] then the diffusion coefficient of HDO appears enhanced (Figure 3d, green ■). For example, in the first 10 min of the reaction the apparent diffusion coefficient for HDO is 2.09×10^{-9} m^2 s^{-1}, compared to 1.78×10^{-9} m^2 s^{-1} after 40
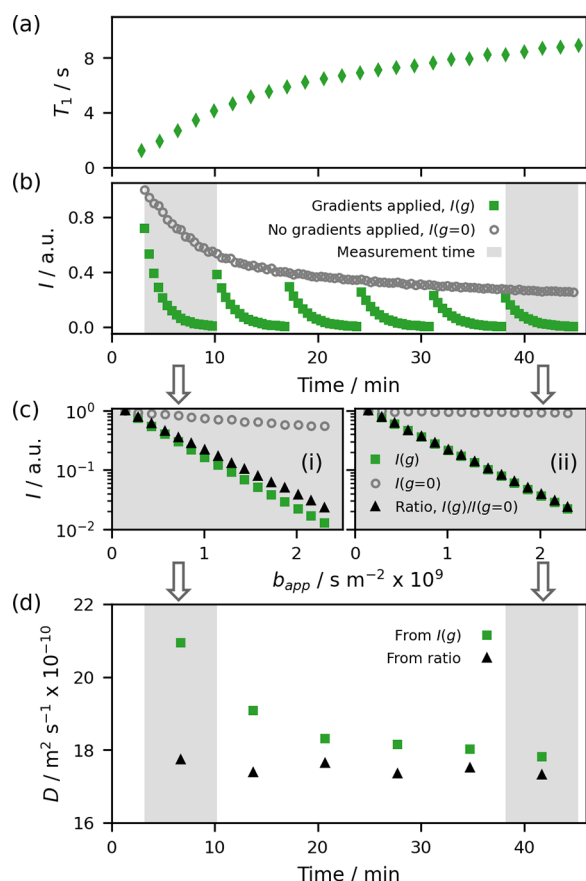
Figure 3. Effect of T_1 changes on the diffusion coefficient during the CuAAC reaction. (a) T_1 of the residual HDO peak during the CuAAC reaction obtained by saturation recovery. (b) Intensity from PGSTE diffusion NMR experiments with (green ■, $I(g)$) and without (○, $I(g = 0)$) magnetic field gradients. (c) Stejskal−Tanner plots for fitting eq 1 for first (i) and last (ii) diffusion experiments. $I(g = 0)$ (○) shows the portion of intensity change due to T_1 changes; dividing the intensities obtained in the presence (green ■) and absence (○) of the applied gradients ($I(g)/I(g = 0)$, ▲) corrects for the T_1 change. (d) Time-resolved diffusion coefficients calculated from the intensity (green ■) or the ratio ($I(g)/I(g = 0)$, ▲). Parameters: 250 mM azide **1**, 250 mM alkyne **2**, 20 mM copper(II) sulfate, 80 mM sodium ascorbate, D_2O; ^1H NMR 400 MHz, PGSTE, δ = 2.5 ms, Δ = 25 ms, and recovery delay during acquisition AQ = 3.15 s.[25]

min. This apparent change of ∼17% in diffusion coefficient is not due to viscosity (SI-10) or temperature changes (SI-11), which both vary <2%. Furthermore, the increase cannot be attributed to convection (SI-8.2).

To isolate the effect of relaxation changes, we repeated the diffusion measurement during the CuAAC reaction with all diffusion gradient amplitudes set to *zero* (SI-1.3; maintaining all other parameters). The data, shown in Figure 3b without gradients (○), reveal a steady decrease in the HDO signal intensity throughout the experiment. This result confirms that a proportion of the signal attenuation during this time is *not* due to the application of diffusion gradient pulses. The Stejskal−Tanner plots of the first and last diffusion measurement (Figure 3c) compare the signal intensities obtained with (green squares) and without (circles) the application of gradient pulses as a function of (apparent) *b*. The ratio of the two ($I(g)/I(g = 0)$, triangles) corresponds to the signal attenuation due to diffusion alone. Fitting this ratio (Figure 3c, triangles) results in the correct, and constant, diffusion

coefficient throughout the reaction (Figure 3d, triangles, see analytical theory SI-13.3). However, this is not the most straightforward method to calculate accurate diffusion coefficients in dynamic systems.

Fortunately, it is possible to accurately determine diffusion coefficients during chemical reactions, despite changes in concentration or relaxation. This is achieved by randomly ordering (shuffling) the gradient pulse amplitudes used in the diffusion NMR experiment. Shuffling the amplitudes removes the correlation between diffusive attenuation and non-diffusion-based intensity changes (SI-8.3).[26,10,17] Here we introduce a list of 500 shuffled gradients where the order of any consecutive 16 gradients has a Pearson correlation coefficient <0.1 (see SI-12.3). This list serves as an example to be used for any time-resolved NMR diffusion experiments. When we apply the shuffled gradient method during the CuAAC reaction, we find no diffusion enhancement for any species (Figure 4a and SI-8.1),[11b] only decreased diffusion.[11a]

The concentration of paramagnetic ions influences the relaxation rates of all species in solution, not just HDO. This can complicate the extraction of *kinetic* data, as signal integrals reflect both concentration and relaxation changes. We see this in the decreasing signal intensity of the residual HDO (Figures 3b and 4b-i), despite no water being consumed in the reaction. The effect is also apparent in the nonconstant sum of integrals for reactant and product signals (Figure 4c-i), resulting in substantially incorrect reaction rates (Figure 4d-i). The signal intensity changes from dynamic relaxation constants can be counteracted by the addition of a paramagnetic relaxation agent, such as organic-soluble chromium(III) acetylacetonate[27] or water-soluble gadolinium−diethylenetriaminepentaacetic acid (Gd-DTPA).[19,20] The paramagnetic relaxation agent must not react or otherwise interfere with the studied reaction. Gadolinium(III) fulfills this requirement for the CuAAC reaction.

In most NMR experiments, an interscan delay of 5 × T_1 is required for complete longitudinal relaxation, which yields maximum signal. More rapid scanning will result in integrals not being strictly proportional to concentration. This will complicate analysis that requires quantitative signal intensities, including diffusion measurements. The incomplete relaxation is no problem for static diffusion NMR measurements, provided a sufficient signal-to-noise ratio is achieved. However, in dynamic systems the signal loss during the recovery delay (where the delay is <5 × T_1) can become problematic. The issue is exemplified in Figure 4b-i, where T_1 of HDO increases from 70 ms to over 5 s, leading to a decrease in signal intensity (here, recovery time 1.5 s). A further complication in PGSTE diffusion experiments is the magnetization lost due to T_1 relaxation during the diffusion time, Δ, which also reduces the signal-to-noise ratio. In cases where $\Delta > T_1$, the loss of magnetization during the diffusion time is very significant; this should be considered when adding a paramagnetic relaxation agent into a system.

For the studied CuAAC reaction, the addition of 230 μM Gd-DTPA to a solution of 250 mM of azide **1** and alkyne **2** in D_2O lowered the T_1 of HDO to 270 ± 50 ms (SI-5.7). Such a short T_1 satisfies the required 5 × T_1 for a relaxation delay of 1.5 s. The addition made no substantial change to the diffusion coefficients throughout the reaction (Figure 4a). However, the intensity of the HDO signal now increases ∼10% throughout the reaction (Figure 5b-ii). This change in intensity is due to the copper catalyzed H−D exchange between the terminal
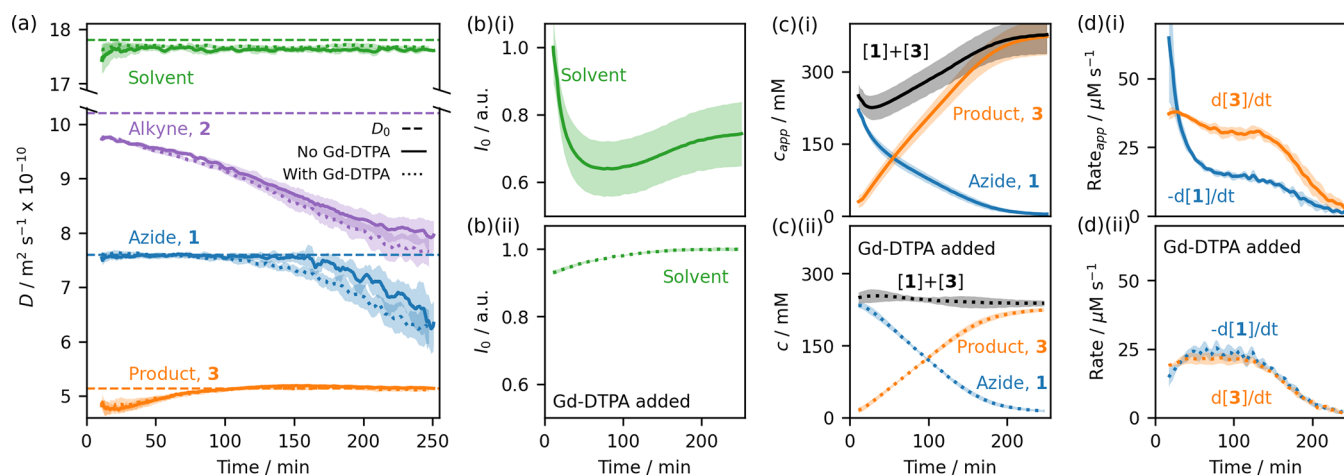
Figure 4. Addition of paramagnetic relaxation agent corrects artifacts from changing T_1. (a) Time-resolved diffusion coefficients of selected peaks during the CuAAC reaction without (solid line) and with Gd-DTPA (dotted line). Dashed lines represent the control diffusion coefficients in 250 mM azide **1**, alkyne **2**, 80 mM sodium ascorbate solution in D_2O (D_0), or after the reaction for the product. (b) Solvent signal intensities (I_0) from diffusion NMR experiments. (c) Apparent concentrations (c_{app}, from I_0) for the CH_2 group in azide **1** and its corresponding position in product **3**. (d) Apparent rates calculated from the concentrations in (c); linear fit applied over every 100 gradient slices (ca. 12 min). (a−d) (i) Without and (ii) with Gd-DTPA. Parameters: 250 mM azide **1**, 250 mM alkyne **2**, 20 mM copper(II) sulfate, 80 mM sodium ascorbate (with 230 μM Gd-DTPA), D_2O; [1]H 500 MHz, PGSTE, δ = 2 ms, Δ = 50 ms, and spoiler recovery delay = 1.5 s. Shaded area represents the standard deviation over three experiments.

alkyne and D_2O, which also causes a decrease in the intensity of the terminal alkyne signal. Deuterium substitution at the terminal position is evidenced by loss of a $^4J_{HH}$ coupling (2.3 Hz) at the propargylic ^{1}H resonance (SI-9.4), and deuterium coupling and intrinsic isotope shifts are observed in the ^{13}C NMR signals of the alkyne (SI-9.3.2).[28]

The Gd-DTPA also affects the relaxation of the CuAAC reactants and product. For example, the T_1 of the methylene protons of azide **1** (in 250 mM azide **1** and alkyne **2** solution) is reduced from 3.8 ± 0.2 s (SI-5.5) without Gd-DTPA to 220 ± 100 ms (SI-5.7) with Gd-DTPA, which fulfills the 5 × T_1 requirement. As a result, the signal intensities more accurately represent the concentrations,[29] allowing reliable reaction kinetics to be determined (Figures 4c-ii and 4d-ii).

While the diffusion coefficients of the residual solvent and reducing agent (sodium ascorbate, SI-8.1) are constant over time, we notice a reproducible decrease in the diffusion coefficient of both reactants during the reaction. The decrease can be partially attributed to the overlap of these peaks with signals for the slower diffusing ascorbate, which worsens as the reaction progresses (Figure 1c and SI-8.5).[11a] To remove this artifact, the experiments were repeated with hydrazine monohydrate as the reducing agent instead of sodium ascorbate. As above, Gd-DTPA was added to allow the collection of accurate kinetic data (Figure 5). These experiments reveal a constant diffusion coefficient for azide **1**, but there is still a decrease of 16 ± 2% for the diffusion coefficient of alkyne **2** after 80 min (Figure 5a) which results from alkyne complexation to copper ions.

Measured diffusion coefficients reflect the weighted average of species that are in fast exchange on the NMR timescale.[30] The fraction of the alkyne bound to copper ions increases during the reaction, and hence the ^{1}H NMR chemical shift of the terminal alkyne moves significantly downfield, consistent with copper binding (Figure 1c and SI-9.2.1).[31] Density functional theory (DFT) studies, following reported protocol,[32] confirmed this shift is expected as the ratio of free to bound alkyne changes (SI-9.1). We also observed the alkyne

^{13}C NMR chemical shifts move downfield during the reaction (SI-9.2.2), consistent with the observation of a weighted average of copper-bound[31c] and free alkyne in solution. Both the ^{1}H and ^{13}C NMR chemical shifts and the diffusion coefficient of the alkyne stop changing once the reaction has reached completion. The opposite chemical shift changes were observed when we titrated free alkyne into a finished reaction, consistent with a changing average environment of free and bound alkyne (SI-9.3).

The ^{1}H and ^{13}C NMR chemical shifts of the product, especially the triazole signal, change during the reaction for the same reason: the signal is the weighted average of the copper-bound and free molecule. The proportion of the product bound to copper is highest when the product concentration is low. The bound fraction decreases as the more product is formed and the weighted average becomes closer to that of the free product. The copper ion likely binds a combination of triazole and alkyne ligands, similar to the commonly used ligand tris((1-benzyl-4-triazolyl)methyl)amine (TBTA) which can be used to stabilize copper(I) during CuAAC reactions.[33] Linewidth analysis during the reaction is also consistent with the expected changing rates of exchange (SI-9.2.1). This analysis shows how a chemical reaction can be monitored by using complementary NMR techniques, including diffusion NMR measurements.

In this study, we have focused on the apparent diffusion enhancement of the CuAAC reaction—the most spectacular of the results presented in a recent report.[8] The other reactions that have been reported showed smaller changes in diffusion coefficients and were subject to the same problematic experimental design and analysis as have been discussed in detail for the CuAAC reaction (e.g., use of monotonically increasing gradient lists and incorrect normalization of diffusion data).[11] Therefore, it is very likely all other reactions examined in the report[8] are affected by the artifacts discussed above, and there is no "boosted mobility" at all.
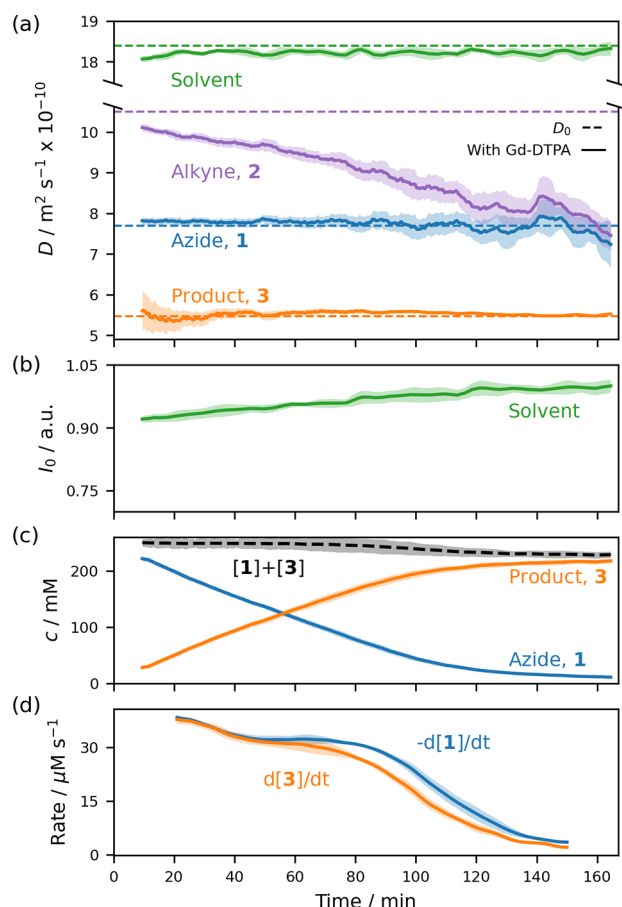
Figure 5. Alternative reducing agent removes NMR signal overlap and reveals evidence of copper complexation. (a) Time-resolved diffusion coefficients of selected peaks during the CuAAC reaction; dashed line is D_0. (b) Solvent signal intensity (I_0) extracted from diffusion NMR experiments. (c) Concentrations (from I_0) for the CH_2 group in azide **1** and its corresponding position in product **3**. (d) Rates calculated from the concentrations in (c) with linear fit applied over every 100 gradient slices (ca. 30 min). Parameters: 250 mM azide **1**, 250 mM alkyne **2**, 20 mM $CuSO_4$, 200 mM hydrazine monohydrate, 230 μM Gd-DTPA, D_2O; ^1H 400 MHz, PGSTE, $\delta = 1$ ms, $\Delta = 10$ ms, and spoiler recovery delay = 0.5 s. Shaded areas represent the standard deviation over three experiments.

CONCLUSION

The addition of a paramagnetic relaxation agent assists accurate measurement of time-resolved diffusion coefficients and reaction kinetics *during* chemical reactions with fluctuating concentrations of paramagnetic ions. The results have been verified by three separate laboratories with different NMR spectrometers, equipped with standard or specialized probes, each using different data acquisition methods, verifying the robust nature of our protocol.

The diffusion NMR methods we present can reveal new insight into well-studied chemical reactions. Here, the observed time-dependent NMR chemical shift and diffusive behavior of the alkyne reactant is consistent with a CuAAC catalytic cycle[34] in which alkyne entry occurs through formation of a discrete copper(I)−alkyne π complex.[35] To the best of our knowledge, this is the first experimental evidence for the precursor to the copper(I) acetylide, whose formation can be rate-determining for the overall cycle.[36]

The methods presented can be used for studying chemical systems where rates of diffusion and chemical reactions are useful parameters, such as polymerizations or supramolecular self-assemblies. Crucially, this study has shown that claims of boosted mobility during chemical reactions have no experimental basis that we could identify. Within experimental error, we show there is no diffusion enhancement at any stage of the reaction above Brownian diffusion. In stark contrast to the claim of 20% diffusion enhancement for the solvent,[8] we find the diffusion coefficient is constant within ±2%.

■ ASSOCIATED CONTENT

ⓢ Supporting Information

The Supporting Information is available free of charge at https://pubs.acs.org/doi/10.1021/jacs.1c09455.

Synthetic procedures, NMR experimental data, spectra and analysis (PDF)

■ AUTHOR INFORMATION

Corresponding Authors

Jonathon E. Beves − *School of Chemistry, UNSW Sydney, Sydney, NSW 2052, Australia;* ⓞ orcid.org/0000-0002-5997-6580; Email: j.beves@unsw.edu.au

Peer Fischer − *Max Planck Institute for Intelligent Systems, 70569 Stuttgart, Germany; Institute of Physical Chemistry, University of Stuttgart, 70569 Stuttgart, Germany;* ⓞ orcid.org/0000-0002-8600-5958; Email: fischer@is.mpg.de

Authors

Lucy L. Fillbrook − *School of Chemistry, UNSW Sydney, Sydney, NSW 2052, Australia;* ⓞ orcid.org/0000-0001-9443-0834

Jan-Philipp Günther − *Max Planck Institute for Intelligent Systems, 70569 Stuttgart, Germany; Institute of Physical Chemistry, University of Stuttgart, 70569 Stuttgart, Germany*

Günter Majer − *Max Planck Institute for Intelligent Systems, 70569 Stuttgart, Germany;* ⓞ orcid.org/0000-0002-5293-4919

Daniel J. O'Leary − *Department of Chemistry, Pomona College, Claremont, California 91711, United States;* ⓞ orcid.org/0000-0002-2887-2957

William S. Price − *Nanoscale Group, School of Science, Western Sydney University, Penrith, NSW 2751, Australia;* ⓞ orcid.org/0000-0002-8549-4665

Hal Van Ryswyk − *Department of Chemistry, Harvey Mudd College, Claremont, California 91711, United States*

Complete contact information is available at:
https://pubs.acs.org/10.1021/jacs.1c09455

Author Contributions

L.L.F. and J.-P.G. contributed to this work equally.

Notes

The authors declare no competing financial interest.
All raw NMR data are freely available on ChemRxiv, DOI: 10.33774/chemrxiv-2021-xpp8v.

■ REFERENCES

(1) (a) Astumian, R. D. Thermodynamics and Kinetics of a Brownian Motor. *Science* **1997**, *276*, 917−922. (b) Hess, H.; Bachand, G. D.; Vogel, V. Powering Nanodevices with Biomolecular Motors. *Chem. - Eur. J.* **2004**, *10*, 2110−2116. (c) Paxton, W. F.; Sundararajan, S.; Mallouk, T. E.; Sen, A. Chemical Locomotion. *Angew. Chem., Int. Ed.* **2006**, *45*, 5420−5429. (d) Goel, A.; Vogel, V. Harnessing Biological Motors to Engineer Systems for Nanoscale Transport and Assembly. *Nat. Nanotechnol.* **2008**, *3*, 465−475. (e) Golestanian, R. Enhanced Diffusion of Enzymes that Catalyze Exothermic Reactions. *Phys. Rev. Lett.* **2015**, *115*, 108102. (f) Zhang, Y.; Hess, H. Chemically-Powered Swimming and Diffusion in the Microscopic World. *Nat. Rev. Chem.* **2021**, *5*, 500−510.

(2) (a) Browne, W. R.; Feringa, B. L. Making Molecular Machines Work. *Nat. Nanotechnol.* **2006**, *1*, 25−35. (b) Kay, E. R.; Leigh, D. A.; Zerbetto, F. Synthetic Molecular Motors and Mechanical Machines. *Angew. Chem., Int. Ed.* **2007**, *46*, 72−191. (c) Abendroth, J. M.; Bushuyev, O. S.; Weiss, P. S.; Barrett, C. J. Controlling Motion at the Nanoscale: Rise of the Molecular Machines. *ACS Nano* **2015**, *9*, 7746−7768. (d) Erbas-Cakmak, S.; Leigh, D. A.; McTernan, C. T.; Nussbaumer, A. L. Artificial Molecular Machines. *Chem. Rev.* **2015**, *115*, 10081−10206. (e) Wilson, M. R.; Solà, J.; Carlone, A.; Goldup, S. M.; Lebrasseur, N.; Leigh, D. A. An Autonomous Chemically Fuelled Small-Molecule Motor. *Nature* **2016**, *534*, 235−240.

(3) Hassan, P. A.; Rana, S.; Verma, G. Making Sense of Brownian Motion: Colloid Characterization by Dynamic Light Scattering. *Langmuir* **2015**, *31*, 3−12.

(4) Visser, A. J. W. G.; Hink, M. A. New Perspectives of Fluorescence Correlation Spectroscopy. *J. Fluoresc.* **1999**, *9*, 81−87.

(5) Price, W. S. *NMR Studies of Translational Motion: Principles and Applications*; Cambridge University Press: Cambridge, 2009.

(6) Günther, J.-P.; Majer, G.; Fischer, P. Absolute Diffusion Measurements of Active Enzyme Solutions by NMR. *J. Chem. Phys.* **2019**, *150*, 124201.

(7) (a) Li, W.; Chung, H.; Daeffler, C.; Johnson, J. A.; Grubbs, R. H. Application of ^{1}H DOSY for Facile Measurement of Polymer Molecular Weights. *Macromolecules* **2012**, *45*, 9595−9603. (b) MacDonald, T. S. C.; Feringa, B. L.; Price, W. S.; Wezenberg, S. J.; Beves, J. E. Controlled Diffusion of Photoswitchable Receptors by Binding Anti-electrostatic Hydrogen-Bonded Phosphate Oligomers. *J. Am. Chem. Soc.* **2020**, *142*, 20014−20020. (c) Zuccaccia, D.; Pinalli, R.; De Zorzi, R.; Semeraro, M.; Credi, A.; Zuccaccia, C.; Macchioni, A.; Geremia, S.; Dalcanale, E. Hierarchical Self-Assembly and Controlled Disassembly of a Cavitand-based Host−Guest Supramolecular Polymer. *Polym. Chem.* **2021**, *12*, 389−401.

(8) Wang, H.; Park, M.; Dong, R.; Kim, J.; Cho, Y.-K.; Tlusty, T.; Granick, S. Boosted Molecular Mobility during Common Chemical Reactions. *Science* **2020**, *369*, 537−541.

(9) (a) Pavlick, R. A.; Dey, K. K.; Sirjoosingh, A.; Benesi, A.; Sen, A. A Catalytically Driven Organometallic Molecular Motor. *Nanoscale* **2013**, *5*, 1301−1304. (b) Dey, K. K.; Pong, F. Y.; Breffke, J.; Pavlick, R.; Hatzakis, E.; Pacheco, C.; Sen, A. Dynamic Coupling at the Ångström Scale. *Angew. Chem., Int. Ed.* **2016**, *55*, 1113−1117.

(10) MacDonald, T. S. C.; Price, W. S.; Astumian, R. D.; Beves, J. E. Enhanced Diffusion of Molecular Catalysts is Due to Convection. *Angew. Chem., Int. Ed.* **2019**, *58*, 18864−18867.

(11) (a) Fillbrook, L. L.; Günther, J.-P.; Majer, G.; Price, W. S.; Fischer, P.; Beves, J. E. Comment on "Using NMR to Test Molecular Mobility during a Chemical Reaction. *J. Phys. Chem. Lett.* **2021**, *12*, 5932−5937. (b) Günther, J.-P.; Fillbrook, L. L.; MacDonald, T. S. C.;

Majer, G.; Price, W. S.; Fischer, P.; Beves, J. E. Comment on "Boosted Molecular Mobility during Common Chemical Reactions". *Science* **2021**, *371*, eabe8322.

(12) (a) Huang, T.; Wang, H.; Granick, S. Reply to Comment on "Using NMR to Test Molecular Mobility during a Chemical Reaction". *J. Phys. Chem. Lett.* **2021**, *12*, 5744−5747. (b) Wang, H.; Park, M.; Dong, R.; Kim, J.; Cho, Y.-K.; Tlusty, T.; Granick, S. Response to Comment on "Boosted Molecular Mobility during Common Chemical Reactions. *Science* **2021**, *371*, eabe8678.

(13) Wang, H.; Huang, T.; Granick, S. Using NMR to Test Molecular Mobility during a Chemical Reaction. *J. Phys. Chem. Lett.* **2021**, *12*, 2370−2375.

(14) Du, J.; Cullen, J. J.; Buettner, G. R. Ascorbic Acid: Chemistry, Biology and the Treatment of Cancer. *Biochim. Biophys. Acta, Rev. Cancer* **2012**, *1826*, 443−457.

(15) Stejskal, E. O.; Tanner, J. E. Spin Diffusion Measurements: Spin Echoes in the Presence of a Time-Dependent Field Gradient. *J. Chem. Phys.* **1965**, *42*, 288−292.

(16) Equation 1 was modified to account for sine-shaped gradient pulses; see ref 5. Price, W. S; Kuchel, P. W Effect of Nonrectangular Field Gradient Pulses in the Stejskal and Tanner (Diffusion) Pulse Sequence. *J. Magn. Reson.* **1991**, *94* (1), 133−139.

(17) MacDonald, T. S. C.; Price, W. S.; Beves, J. E. Time-Resolved Diffusion NMR Measurements for Transient Processes. *ChemPhysChem* **2019**, *20*, 926−930.

(18) Bloembergen, N.; Purcell, E. M.; Pound, R. V. Relaxation Effects in Nuclear Magnetic Resonance Absorption. *Phys. Rev.* **1948**, *73*, 679−712.

(19) Strich, G.; Hagan, P. L.; Gerber, K. H.; Slutsky, R. A. Tissue Distribution and Magnetic Resonance Spin Lattice Relaxation Effects of Gadolinium-DTPA. *Radiology* **1985**, *154*, 723−726.

(20) Heffern, M. C.; Matosziuk, L. M.; Meade, T. J. Lanthanide Probes for Bioresponsive Imaging. *Chem. Rev.* **2014**, *114*, 4496−4539.

(21) Over time some of this copper(I) will be oxidized to copper(II) due to exposure to air.

(22) Vold, R. L.; Waugh, J. S.; Klein, M. P.; Phelps, D. E. Measurement of Spin Relaxation in Complex Systems. *J. Chem. Phys.* **1968**, *48*, 3831−3832.

(23) Within error of the value for 20 mM copper sulfate in D_2O, 69 ± 1 ms; see SI-5.3.

(24) In a D_2O solution containing just 20 mM sodium ascorbate, the T_1 value of HDO was 44 ± 4 s (SI-5.4), illustrating significant T_1 changes other than by paramagnetic species (see Tables S3 and S4 for a full summary of T_1 constants in static solutions).

(25) We included an analytical theory to estimate the magnitude of such effects (see SI-13.3).

(26) (a) Oikonomou, M.; Asencio-Hernández, J.; Velders, A. H.; Delsuc, M.-A. Accurate DOSY Measure for Out-of-Equilibrium Systems using Permutated DOSY (p-DOSY). *J. Magn. Reson.* **2015**, *258*, 12−16. (b) Urbańczyk, M.; Bernin, D.; Czuroń, A.; Kazimierczuk, K. Monitoring Polydispersity by NMR Diffusometry with Tailored Norm Regularisation and Moving-Frame Processing. *Analyst* **2016**, *141*, 1745−1752.

(27) Gansow, O. A.; Burke, A. R.; La Mar, G. N. A Shiftless Relaxation Reagent for Carbon-13 Magnetic Resonance of Organometallic Carbonyl Compounds. *J. Chem. Soc., Chem. Commun.* **1972**, 456−457.

(28) (a) Shoolery, J. N.; Johnson, L. F.; Anderson, W. A. The High Resolution nmr Spectrum of Methyl Acetylene. *J. Mol. Spectrosc.* **1961**, *5*, 110−117. (b) Wigglesworth, R. D.; Raynes, W. T.; Kirpekar, S.; Oddershede, J.; Sauer, S. P. A. Nuclear Magnetic Shielding in the Acetylene Isotopomers Calculated from Correlated Shielding Surfaces. *J. Chem. Phys.* **2000**, *112*, 736−746.

(29) The relationship between I_0 and relaxation constants T_1 and T_2 is nontrivial. For a discussion of the simpler PGSE sequence, see: Lee, A. M.; Stait-Gardner, T.; Price, W. S. Explicit phenomenological solutions for magnetization exposed to an arbitrary NMR diffusion steady state pulse sequence. *J. Chem. Phys.* **2021**, *155*, 144204.

(30) (a) Kärger, J. Zur Bestimmung der Diffusion in einem Zweibereichsystem mit Hilfe von gepulsten Feldgradienten. *Ann. Phys. (Berlin, Ger.)* **1969**, *479*, 1−4. (b) Melchior, J.-P.; Majer, G.; Kreuer, K.-D. Why do Proton Conducting Polybenzimidazole Phosphoric Acid Membranes Perform Well in High-Temperature PEM Fuel Cells? *Phys. Chem. Chem. Phys.* **2017**, *19*, 601−612. (c) Wijesekera, D.; Stait-Gardner, T.; Gupta, A.; Chen, J.; Zheng, G.; Torres, A. M.; Price, W. S. A Complete Derivation of the Kärger Equations for Analyzing NMR Diffusion Measurements of Exchanging Systems. *Concepts Magn. Reson., Part A* **2018**, *47A*, e21468.

(31) (a) Reger, D. L.; Huff, M. F. (Alkyne) (2,2′-bipyridine)copper (I) Complexes. Controlled Formation of $[Cu(bpy)(alkyne)]^+$ and $\{[Cu(bpy)]_2(alkyne)\}^{2+}$. *Organometallics* **1992**, *11*, 69−73. (b) Oztopcu, O.; Mereiter, K.; Puchberger, M.; Kirchner, K. A. Tri- and Tetracoordinate Copper(I) Complexes Bearing Bidentate Soft/Hard SN and SeN Ligands Based on 2-aminopyridine. *Dalton Trans.* **2011**, *40*, 7008−7021. (c) Martin, C.; Sierra, M.; Alvarez, E.; Belderrain, T. R.; Perez, P. J. Hydrotris(3-mesitylpyrazolyl)borato-copper(I) Alkyne Complexes: Synthesis, Structural Characterization and Rationalization of their Activities as Alkyne Cyclopropenation Catalysts. *Dalton Trans.* **2012**, *41*, 5319−5325.

(32) Jain, R.; Bally, T.; Rablen, P. R. Calculating Accurate Proton Chemical Shifts of Organic Molecules with Density Functional Methods and Modest Basis Sets. *J. Org. Chem.* **2009**, *74*, 4017−4023.

(33) Chan, T. R.; Hilgraf, R.; Sharpless, K. B.; Fokin, V. V. Polytriazoles as Copper(I)-Stabilizing Ligands in Catalysis. *Org. Lett.* **2004**, *6*, 2853−2855.

(34) Worrell, B. T.; Malik, J. A.; Fokin, V. V. Direct Evidence of a Dinuclear Copper Intermediate in Cu(I)-Catalyzed Azide-Alkyne Cycloadditions. *Science* **2013**, *340*, 457−460.

(35) For examples of static NMR diffusion studies of reactive intermediates, see: (a) Li, D.; Keresztes, I.; Hopson, R.; Williard, P. G. Characterization of Reactive Intermediates by Multinuclear Diffusion-Ordered NMR Spectroscopy (DOSY). *Acc. Chem. Res.* **2009**, *42*, 270−80. (b) Schlorer, N. E.; Cabrita, E. J.; Berger, S. Characterization of Reactive Intermediates by Diffusion-Ordered NMR Spectroscopy: a Snapshot of the Reaction of $^{13}CO_2$ with $[Cp_2Zr(Cl)H]$. *Angew. Chem., Int. Ed.* **2002**, *41*, 107−109.

(36) (a) Rodionov, V. O.; Fokin, V. V.; Finn, M. G. Mechanism of the Ligand-Free Cu-I-Catalyzed Azide-Alkyne Cycloaddition Reaction. *Angew. Chem., Int. Ed.* **2005**, *44*, 2210−2215. (b) Kuang, G. C.; Guha, P. M.; Brotherton, W. S.; Simmons, J. T.; Stankee, L. A.; Nguyen, B. T.; Clark, R. J.; Zhu, L. Experimental Investigation on the Mechanism of Chelation-Assisted, Copper(II) Acetate-Accelerated Azide-Alkyne Cycloaddition. *J. Am. Chem. Soc.* **2011**, *133*, 13984−14001. (c) Seath, C. P.; Burley, G. A.; Watson, A. J. Determining the Origin of Rate-Independent Chemoselectivity in CuAAC Reactions: An Alkyne-Specific Shift in Rate-Determining Step. *Angew. Chem., Int. Ed.* **2017**, *56*, 3314−3318.